Real-time X-ray radioscopy on metallic foams using a compact micro-focus source

Francisco García Moreno[1,2], Michael Fromme[1], and **John Banhart[1,2]**
[1]Hahn-Meitner-Institut Berlin, Berlin, Germany
[2]Technical University Berlin, Berlin, Germany

A measurement apparatus for observing the foaming of metals is described. It consists of a microfocus X-ray source, a small heater and a panel detector. The foaming of samples can be recorded in real-time with frequencies up to 16 Hz and resolutions down to 5 μm due to the small spot size. Magnifications up to 10× are obtained by simply changing the distance between source, sample and detector. Foaming of Al alloys and sandwiches was investigated applying different heating rates and final foaming temperatures. An image analysis program was used to automatically recognise and count the rupture of cell walls during foaming.

1 Introduction

Advancement of metal foam technology calls for an improvement of foam properties and a closer process control, which requires more knowledge about the physics of metal foaming. In order to understand, e.g., the nucleation kinetics of the blowing agent, the influence of its pre-treatment or the kinetics of pore growth, non-destructive methods such as X-ray radioscopy [1] and tomography [2] were proposed and successfully applied. X-ray radioscopy has been proved a powerful tool for real-time diagnostics, not only for the foaming process, but also for observing liquid metals [3,4], metal solidification [5], or flaw detection in Al castings [6]. We present an X-ray tool for characterising metal foams and analysing the influence of process parameters.

2 Real-time X-ray radioscopy

The foam characterisation tool built is shown in Fig. 1. The imaging system consists of a closed, air-cooled microfocus (5-50 μm) X-ray source from Hamamatsu with up to 150 kV and 500 μA (75 W) and a flat panel detector (area ~ 120×120 mm^2, 2240×2368 $pixel^2$, pixel size: 50 μm) also from Hamamatsu. The maximum acquisition rate is 16 pictures/s. Two main differences of such a measurement system in comparison to the imaging with a synchrotron beam previously used [1] have to be considered: First, the X-ray intensity of a microfocus source is smaller than of a synchrotron source. In our measurement configuration the intensity is enough to get satisfactory contrast for many applications, even for real-time picture acquisition. Secondly, we have a divergent beam instead of a parallel one when using a point source (see Fig. 2).This type of projection is described in detail e.g. by Mery et al. [4]. One implication is the possibility to adjust the required magnification M. It is given by M = b/a (a is the distance between source and sample and b between source and detector). Useful M's can be as high as 10 for our configuration. To find the best imaging parameters with, e.g., the best spatial and time resolution and the desired magnification other factors have to be considered such as the sample geometry, the source pitch ($d_{source} \approx 5$ μm), the detector pitch ($d_{detec} = 50$ μm) or the divergence distortion $d_{div} \approx t \cdot h/4 \cdot a$ for $t << a$. At a given magnification a higher distance

between source and detector will reduce d_{div}, but the intensity will be also reduced as $I \sim 1/b^2 \sim 1/M^2$. The parameters selected for the following experiments were: 100 kV, 100 μA, a = 120 mm, b = 500 mm, M = 4, t_0 = 10 mm, h_0 = 4-5 mm, l_0 = 15-20 mm. The obtained high resolution X-ray images have a size of 2240×2368 pixel^2 per image and are acquired at 0.5 pic/s. In this case the resolution R is limited by the pitch of the detector: $R = d_{detect}/M$ = 12.5 μm. The maximum distortion $d_{div} \approx$ 0.1 mm is around 2% of the sample height which is not disturbing for pore analysis.

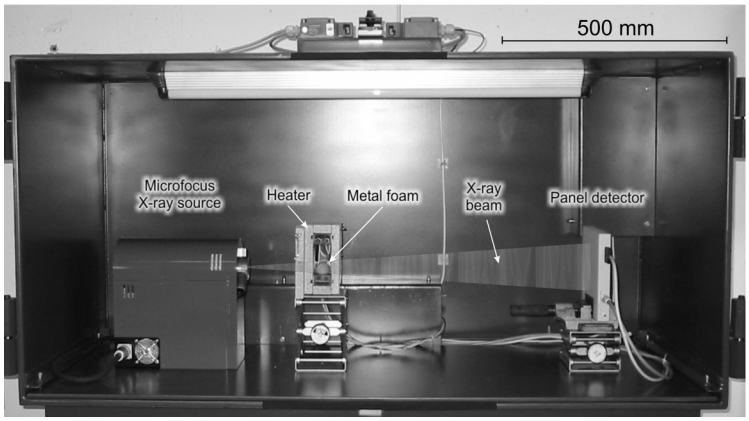

Fig. 1. X-ray radioscopy measurement apparatus

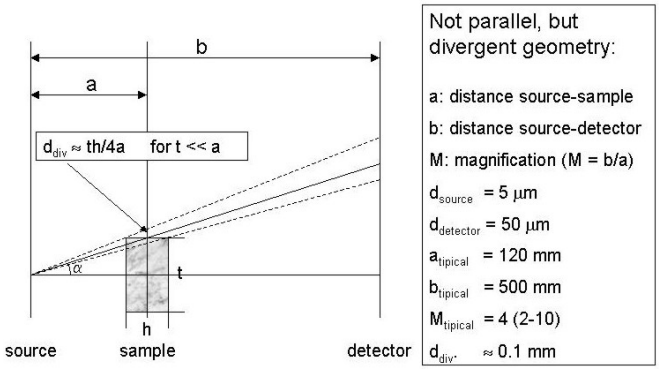

Fig. 2. Imaging geometry

The most common way of foaming is to introduce the foamable material into a pre-heated furnace with a large heat capacity. Hereby the foam temperature increases rapidly, whereas the furnace temperature stays more or less constant. The temperature course cannot be influenced. In contrast, the two heater systems used in our experiments are heated up together with the sample to the desired temperature T_{end}, allowing us to apply different temperature profiles. The resistive heater (~ 2 kW) consists of two heating plates, with a path for the X-ray beam in between through side walls made of 2×0.25 mm Al-foil + 2×0.05 stainless steel-foil with a low X-ray absorption. Free foaming or foaming inside

a mould is possible. The second heater is an IR-lamp heater containing three 150 W halogen lamps. This is a simple open construction without absorption in the beam direction. Due to the inhomogeneous temperature distribution by the lamps only foaming in a mould is useful.

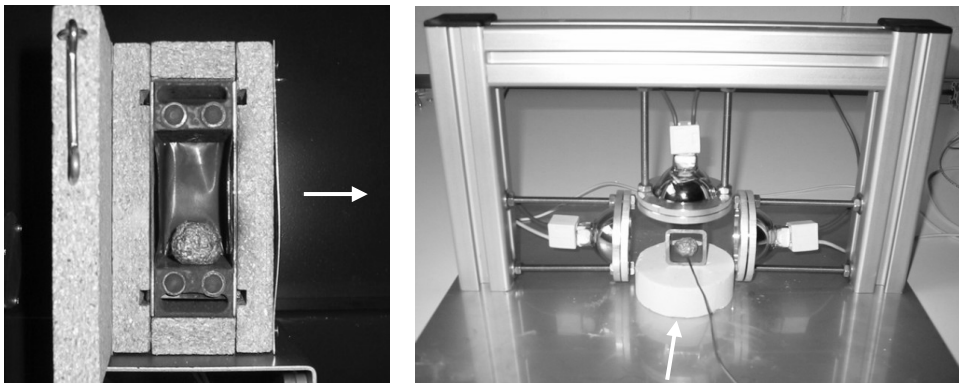

Fig. 3. Resistive (left) and IR-lamp heater (right). The arrows define the beam direction.

3 Methods for image analysis

A computer analysis software based on the PV-WAVE program [7] was developed to process the acquired images, calculate the height and expansion of the foams and to analyse cell rupture events. This program is able to separate darker object pixels from brighter pixels above and beneath the object and from black pixels of the supporting surface in a first step. The object pixels cannot be separated from the environment by fixed threshold criteria. Thermal expansion effects of the substrate are corrected easily.

In a second step consecutive images are compared. Abrupt changes in pixel values correspond to modified material thickness. To separate thermal noise from real cell wall rupture events, several filters are applied to the differential images, such as threshold, median, and dilation. The remaining pixels of interest are analysed for clusters. When foam growth has slowed down, these clusters correspond to collapsing bubbles and we can obtain information about where and when these events take place.

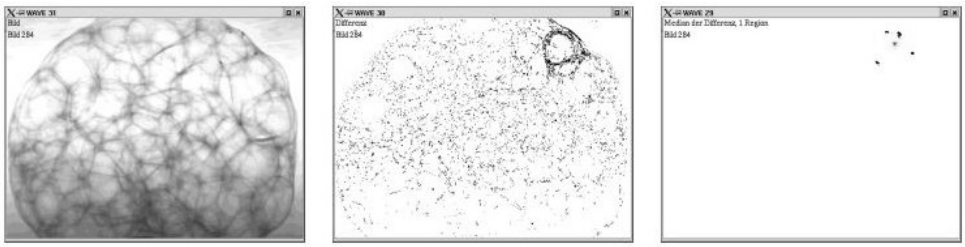

Fig. 4. Analysis software: single radioscopic picture (left), difference between two following pictures (middle), and cell wall rupture event identification (right).

4 Results and discussion

A foamable AlSi6Cu4 alloy and a sandwich panel were foamed. The corresponding radioscopic images are compared and analysed. Results obtained by varying the final foaming temperature and the heating rate to this temperature are presented and discussed.

4.1 Foam expansion dynamic

Al/AlSiCu/Al-sandwich material from ALM was foamed at different temperatures (see Fig. 5, left). The temperature was measured directly inside the sample by a thermocouple. During melting and foaming the system temperature reaches a plateau or even drops because of the small heat capacity of our heaters.

Fig. 5, right, shows the expansion kinetics of these samples. Before reaching the melting point only thermal expansion can be observed. After the melting point has been reached and while the blowing gas supply is not exhausted, expansion takes place very rapidly. After this a slight contraction was observed for almost all the samples, corresponding to internal processes such as coarsening. The maximal expansion as well as the expansion velocity are increased with increasing temperatures, but the foams become unstable (e.g. T = 650°C) due to increasing coarsening, cell wall rupture and drainage. Finally the upper face sheet melts and the sandwiches collapse abruptly.

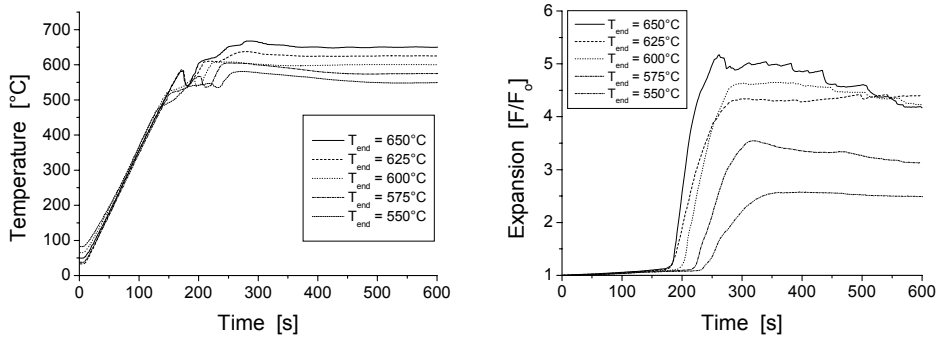

Fig. 5. Temperature evolution (left) and foam expansion evolution (right) for ALM Al/AlSiCu/Al-sandwich

4.2 Temperature ramps

The heating system used permits choosing variable heating rates. For AlSi6Cu4 the range of 33.3 – 133,3 K/min was analysed (see Fig. 6). The samples foamed at 66,6-133,3 K/min have very similar expansion curves, reaching the same maximum expansion, but shifted in time. This shift is obviously a result of the delay in reaching the melting temperature (~ 560 °C). The sample heated at 33,3 °/min exhibits an expansion maximum of only 75% of the other samples and a more rapid decrease of sample height after foaming. A critical heating rate seems to exist, below which expansion does not reach its maximum. Possibly losses of hydrogen during heating or increasing oxidation are the reason. Fig. 6. contains 2 radiographs extracted from the image sequence and shows the

fully expanded foams produced at different heating rates. For 33.3 K/min, beside a reduced expansion, heterogeneities in pore sizes and distribution are visible.

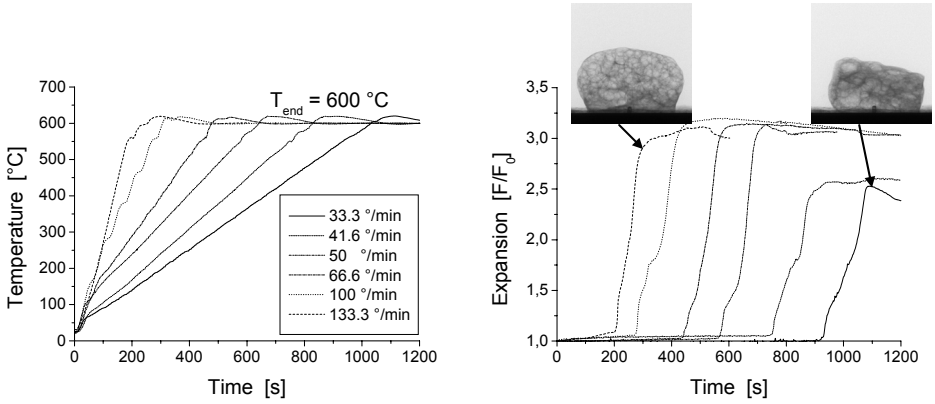

Fig. 6. Different temperature ramps by AlSi6Cu4-foam (left) and the corresponding expansion behaviour (right) with radiographs of the fully expanded foam

4.3 Cell wall rupture

To observe the stability of the foams, cell wall rupture was analysed quantitatively. As for freely foaming samples there is the disadvantage of a slowly moving contour, it is difficult for the software to distinguish between this motion and cell rupture. Although this problem was solved, foaming in a mould was found to be a more appropriate, since in this there is less ambiguity in the analysis.

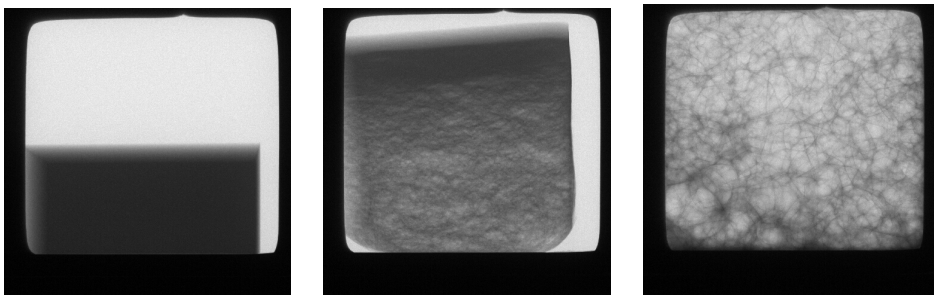

Fig. 7. Heating phase (left), expansion phase (middle) and coarsening phase (right) of an Al-foam in a mould produced with the resistive heater

Fig. 7 demonstrates that in the expansion absorption contrast changes due to massive pore formation and growth. The expansion begins at the bottom (see Fig. 7 middle), close to the resistive heater. Using the IR-lamp heater the upper and side walls of the mould are hotter than the bottom wall and foaming begins earlier on these sides. Only after the expansion phase is over and coarsening begins the analysis can be started.

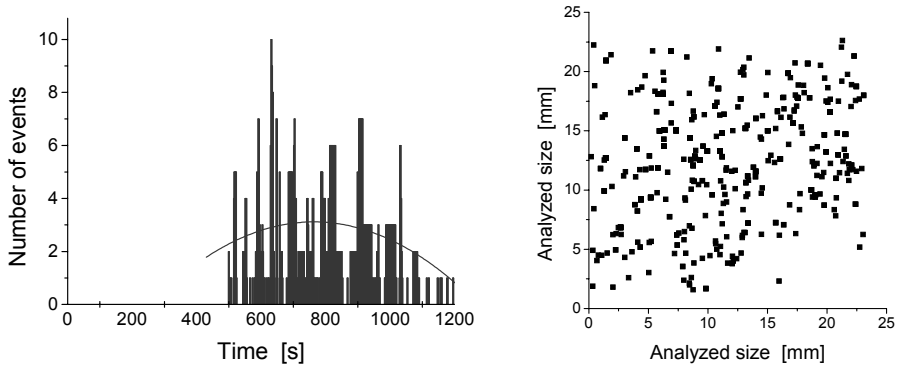

Fig. 8. Time (left) and spatial (right) cell wall rupture event distribution in an Al 99.7 foam in a mould (see Fig. 8.)

The distribution of the rupture events as a function of time as obtained by image analysis is shown in Fig. 8, corresponding to the sample in Fig. 7. A total of 583 events with a time resolution of 2 s were registered in the measuring interval. After expansion has come to an end the number of events increases in time and drops again after several minutes. This distribution has a maximum at ~730 s. The spatial distribution of events is quite uniform except in the lower-right region where no events could be registered. This can be the result of gravitational drainage supplying metal to the metal films and preventing them to reach the critical thickness and to rupture.

5 Conclusions

We developed a X-ray radioscopy measurement apparatus for in-situ examinations of the foaming process of metals. Different heater configurations were tested and different heating rates applied. In combination with an image analysis software the kinetics of foam expansion and cell wall rupture could be quantified. Foam instability during expansion of Al-sandwiches at 650 °C was found, as well as a reduced maximum expansion and rapid collapse for AlSi6Cu4 at $dT/dt \leq 33{,}3$ K/min. Cell wall rupture events in a mould were found to have a maximum in time and be uniformly distributed in space.

Acknowledgement: DFG (grant Ba 1170/3-2) and ESA (contract 14308) supported this work. Samples were provided by ALM GmbH and Schunk Sintermetalltechnik.

References

[1] J. Banhart, H. Stanzick, L. Helfen, T. Baumbach, K. Nijhof, Adv. Eng. Mat. **3**, 407 (2001)
[2] A. Rack, A. Haibel, B. Matijasevic, J. Banhart, these proceedings, 295-300
[3] J. N. Koster, T. Seidel, R. Derebail, J. Fluid Mech. **29**, 343 (1997)
[4] P. D. Lee, J. D. Han, Acta Mater. **45**, 4155 (1997)
[5] P. A. Curreri, and W. F. Kaukler, Met.Trans. A, **27**A, 801 (1996)
[6] D. Mery, and D. Filber, IEEE Trans.on Robotics and Automation **18,** 890 (2002)
[7] PV-Wave, Visual Numerics, http://www.vni.com/products/wave/